DALTON
FULL PAPER

# Syntheses, crystal structures and properties of mononuclear chromium(III) and dinuclear vanadium(III) and copper(II) complexes with a bis-bipyridyl ligand †

**Craig M. Grant,[a] Brian J. Stamper,[a] Michael J. Knapp,[b] Kirsten Folting,[a] John C. Huffman,[a] David N. Hendrickson*[b] and George Christou*[a]**

[a] *Department of Chemistry and the Molecular Structure Center, Indiana University, Bloomington, IN 47405-7102, USA*
[b] *Department of Chemistry, University of California at San Diego, La Jolla, CA 92093-0358, USA*

***Received 30th June 1999, Accepted 4th August 1999***

The reaction between $[VCl_3(thf)_3]$ and the bis-bidentate ligand L [L = 1,2-bis(2,2′-bipyridyl-6-yl)ethane] in MeOH gave the oxo-bridged dinuclear complex $[V_2OCl_2L_2]Cl_2$ **1**, which contains a near linear V–O–V unit. Reaction of $CrCl_3·6H_2O$ with L in refluxing MeOH gave mononuclear *trans*-$[CrCl_2L]Cl$ **2** with the ligand L co-ordinated equatorially. Equimolar reaction of L with $[Cu_2(OAc)_4(H_2O)_2]$ in EtOH followed by addition of $NaClO_4$ yielded the dinuclear complex $[Cu_2(OAc)_{2.4}(OEt)_{0.6}L]ClO_4$ **3**, whose cation contains a $[Cu_2(OAc)_2(OAc_{0.4}/OEt_{0.6})]^+$ core, with two bridging $OAc^-$ ligands and a bridging oxygen atom shared by disordered $OEt^-$ and monodentate $OAc^-$ ligands. The analogous reaction with addition of $HBF_4$ gave $[Cu_2F(OAc)_2L]BF_4$ **4**, which contains two bridging $OAc^-$ ligands and a bridging $F^-$ atom. Compound **1** shows strong ferromagnetic coupling between vanadium(III) ions with $J > 100$ $cm^{-1}$ resulting in only the $S = 2$ ground state being populated, whereas **4** shows weak ferromagnetic coupling, $J \approx +8$ $cm^{-1}$ ($H = -2JS_iS_j$ convention) and a $S = 1$ ground state.

We have long been interested in the synthesis of polynuclear transition metal complexes using a variety of bridging and chelating ligands. A wide range of nuclearities and structural types have been obtained, including $Mn_4$,[1] $Mn_{10}$,[2] $Mn_{11}$,[3] $Co_4$,[4] and $Ni_4$[5] by combining carboxylate ligands with simple chelates such as $dbm^-$ and bpy ($dbm^-$ is the anion of dibenzoylmethane; bpy = 2,2′-bipyridine). In most cases, the metal ions are held together by one or more types of O-based bridging groups such as $O^{2-}$, $OH^-$, $OR^-$ and $RCO_2^-$. More recently we have extended these studies to include oligo-bipyridyl ligands to investigate to what extent the use of such ligands might affect the identity of obtained products compared with normal bpy and to what extent this might thus prove a route to new cluster types. Initial investigations employing metal carboxylates and the bis-bipyridyl ligand L [L = 1,2-bis(2,2′-bipyridyl-6-yl)ethane][6] have led to interesting new high nuclearity species, including the mixed valence octanuclear cobalt complex $[Co_8O_4(OH)_4(OAc)_6L_2][ClO_4]_2$,[7] tetranuclear manganese complex $[Mn_4O_2(OAc)_4L_2][ClO_4]_2$,[8] and the hexanuclear iron species $[Fe_6O_4Cl_4(O_2CPh)_4L_2][FeCl_4]_2$.[9] Investigations with L and other transition metals have also proven interesting and our initial studies with vanadium(III), chromium(III) and copper(II) are herein reported. The synthesis and structural characterisation of mononuclear (Cr) and three dinuclear complexes (V and 2 Cu) are presented and compared and contrasted with the known complexes formed by bpy. The magnetic characterisation of the linear oxo-bridged vanadium(III) and fluoro-bridged copper(II) dinuclear complexes is also described.

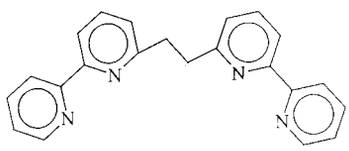

L

† *Supplementary data available*: rotatable 3-D crystal structure diagram in CHIME format. See http://www.rsc.org/suppdata/dt/1999/3399/

## Experimental

### General

All manipulations involving vanadium(III) were performed under a purified argon atmosphere employing standard Schlenk and glove-box techniques. Methanol and diethyl ether were distilled under argon from magnesium methoxide and sodium–benzophenone solutions, respectively. The compounds $[VCl_3(thf)_3]$[10] and L[6] were prepared by published literature procedures. All other starting materials were used as received. Solvents used in the synthesis of **2**, **3** and **4** were used without further purification.

**CAUTION:** perchlorate salts are potentially explosive. Although no detonation tendencies have been observed in this work, caution is advised and handling of only small quantities is recommended.

### Preparations

**$[V_2OCl_2L_2]Cl_2$ 1.** A green MeOH (30 ml) solution of $[VCl_3(thf)_3]$ (0.579 g, 1.55 mmol) was added to L (0.523 g, 1.55 mmol) to afford a red-orange solution that became more intense over the course of several minutes; after 2–3 h it was intense purple. The solution was stirred for 10 h. Vapour diffusion of $Et_2O$ into it produced after one week large purple-black crystals of compound **1**·6MeOH suitable for crystallography. The crystals were collected by filtration and dried *in vacuo*. The yield was 0.378 g (49%) based on vanadium; dried solid analysed as **1**·MeOH·$2H_2O$ (Found: C, 53.72; H, 4.29; N, 11.34. $C_{44}H_{36}Cl_4N_8OV_2$·MeOH·$2H_2O$ requires C, 53.80; H, 4.41; N, 11.15%). Selected IR spectral data (KBr, $cm^{-1}$): 1601vs, 1565s, 1491m, 1454vs, 1412m, 1302m, 1259m, 1238w, 1188w, 1159m,

1091m, 1055w, 1022vs, 939w, 825m, 775vs, 725vs, 653m, 642m, 563w and 449w. Electronic spectral data in MeOH [$\lambda_{max}$/nm ($\varepsilon$/$M^{-1}$ $cm^{-1}$)]: 244 (35195), 308 (36745), 560 (7914) and 624 (5130).

**[$CrCl_2L$]Cl 2.** One equivalent of L (0.22 g, 0.65 mmol) was added to a MeOH (20 ml) solution of hydrated chromium chloride (0.17 g, 0.65 mmol). The resultant light green solution was heated to reflux for 18 h during which time it darkened. Slow evaporation over 7 d afforded green crystals of compound **2**·2MeOH suitable for crystallography. The yield was 0.148 g (41% yield) based on Cr; dried solid analysed as **2**·0.5MeOH·$2H_2O$ (Found: C, 48.87; H, 4.17; N, 9.72. $C_{22}H_{18}Cl_3CrN_4$·0.5MeOH·$2H_2O$ requires C, 49.24; H, 4.41; N, 10.21%). Selected IR spectral data (KBr, $cm^{-1}$): 1603vs, 1564s, 1495s, 1458vs, 1415m, 1302m, 1259w, 1244w, 1186w, 1165m, 1113w, 1093w, 1057w, 1030s, 1020s, 941w, 916w, 891w, 825m, 779vs, 727m, 655m, 642m, 563w and 459s.

**[$Cu_2(OAc)_{2.4}(OEt)_{0.6}L$]$ClO_4$ 3.** The compound [$Cu_2(OAc)_4(H_2O)_2$] (0.12 g, 0.30 mmol) was added to a warm yellow EtOH (40 ml) solution of L (0.10 g, 0.30 mmol). This dark green solution was stirred for 30 min, and $NaClO_4$ (0.036 g, 0.29 mmol) dissolved in EtOH (5 ml) added. Slow evaporation over 10 d produced a mixture of blue and green crystals. Small samples of each were separated manually, and IR spectroscopic examination confirmed the blue compound to be the previously reported mononuclear species [CuL]$ClO_4$.[6] Subsequent extraction of the mixture with MeCN left only green crystals of **3**, which were collected by filtration, washed with $Et_2O$ and dried *in vacuo*. The yield was low (*ca*. 20%) and dried solid analysed as **3**·$3H_2O$ (Found: C, 42.26; H, 3.66; N, 7.21. $C_{28}H_{28.2}ClCu_2N_4O_{9.4}$·$3H_2O$ requires C, 42.66; H, 4.38; N, 7.11%). Selected IR spectral data (KBr, $cm^{-1}$): (green crystals) 1668m, 1591vs, 1572s, 1495m, 1454s, 1431s, 1408m, 1307w, 1280m, 1172w, 1153w, 1087vs (br) ($ClO_4$), 1030m, 1014m, 788m, 655w, 640w and 623m; (blue crystals) 1604m, 1576w, 1498m, 1460s, 1437w, 1421w, 1304w, 1259w, 1232w, 1163w, 1103vs (br) ($ClO_4$), 1032m, 1018m, 825w, 783s, 729w, 646w and 625s.

**[$Cu_2F(OAc)_2L$]$BF_4$ 4.** Hydrated copper acetate (0.26 g, 0.65 mmol) was added to a warm yellow MeOH (40 ml) solution of L (0.22 g, 0.66 mmol). This dark green solution was stirred while being allowed to cool for 30 min and then 1 equivalent of $HBF_4$·$Et_2O$ (100 μl, 0.58 mmol) was added resulting in an immediate change to light blue. Blue-green crystals formed from the undisturbed solution over a 12 h period in 44% yield (0.20 g); dried solid analysed as **4**·$H_2O$ (Found: C, 44.44; H, 3.76; F, 13.34; N, 7.86. $C_{26}H_{24}BCu_2F_5N_4O_4$·$H_2O$ requires C, 44.15; H, 3.71; N, 7.92; F, 13.43%). Selected IR spectral data (KBr, $cm^{-1}$): 1591vs, 1572 (sh), 1495m, 1454vs, 1423s, 1348w, 1315m, 1305m, 1263w, 1236w, 1172m, 1155m, 1055s (br) ($BF_4^-$), 831w, 798s, 785vs, 729w, 679w, 657s, 640s, 617w, 520w, 445w and 428w.

### X-Ray crystallography

Data for all complexes were collected at low-temperature on a Picker four-circle diffractometer with graphite-monochromated Mo-Kα radiation (λ 0.710 69 Å); details of the diffractometry, low temperature facilities, and computational procedures employed by the Molecular Structure Center are available elsewhere.[11a] Data collection and structure solution information are listed in Table 1. Data were corrected for Lorentz-polarisation effects, and equivalent data were averaged. In addition, absorption corrections were applied to the data of **2** and **4**. The structures were solved by a combination of direct methods (SHELXTL[11b] or MULTAN[11c]) and standard Fourier techniques, and refined on *F* by full-matrix least-squares cycles.

Complex **1**·6MeOH crystallizes in monoclinic space group $P2_1/n$. In addition to the cation and anions, six full-weight occupancy MeOH solvate molecules were located. Two of these were disordered but refined without problem. All non-hydrogen atoms (excluding those of disordered solvent molecules) were refined using anisotropic thermal parameters. Hydrogen atoms were introduced in fixed calculated positions in the final cycles of refinement. The full unique data set was used for the refinement (on *F*); reflections having $F < 3.0\sigma(F)$ were given zero weight. A final Fourier-difference map was essentially featureless, the largest peak was 0.94 e $Å^{-3}$ and the deepest hole was −0.57 e $Å^{-3}$.

Complex **2**·2MeOH crystallizes in orthorhombic space group *Pbca*. The structure was solved without problem and all non-hydrogen atoms, including two well behaved MeOH solvate molecules were refined anisotropically. Hydrogen atoms were located and refined as isotropic contributors in the final cycles of refinement. A final Fourier-difference map was featureless, the largest peak being less than 0.4 e $Å^{-3}$.

Complex **3** crystallizes in monoclinic space group $P2_1/c$. The location of the atoms surrounding O(37) was difficult. A dangling monodentate $OAc^-$ was expected from spectroscopic evidence (IR) but the initial difference map seemed to indicate a bridging $OEt^-$ group and it subsequently became clear that a $OEt^-/OAc^-$ disorder was present. Fourier-difference maps were used to resolve the disorder and a satisfactory model was obtained and the structure refined. For the particular crystal studied the composition of the disorder was 60% $OEt^-$ [O(37)–C(39)] and 40% $OAc^-$ [O(37) and C(40)–C(42)]. The atoms involved in the disorder [C(38)–C(42)] were refined using isotropic thermal parameters; all other non-hydrogen atoms were refined anisotropically. Hydrogen atoms (except on the disordered atoms) were introduced in fixed, calculated positions. The full unique data set was used for the refinement (on *F*); reflections having $F < 3.0\sigma(F)$ were given zero weight. A final Fourier-difference map was essentially featureless, the largest peak was 0.93 e $Å^{-3}$, 0.96 Å from C(30), and the deepest hole was −0.89 e $Å^{-3}$.

Complex **4** crystallizes in triclinic space group $P\bar{1}$. A disorder was present in the ethylene bridge and two adjacent carbon atoms in the aromatic ring of the ligand [C(24), C(25), C(27) and C(28) respectively], but this was readily resolved. In addition to the cation and $BF_4^-$ anion, a badly disordered solvent molecule was located, and it was modeled by three partial occupancy atoms [O(43), O(44) and C(45)] that lie in close proximity to each other suggesting a disordered MeOH molecule. Hydrogen atoms (with the exception of those associated with the disorder and solvent) were located and refined as isotropic contributors in the final cycles of refinement. The final Fourier-difference map was essentially featureless, the largest peaks being less than 0.7 e $Å^{-3}$ in the vicinity of the disordered solvent molecule.

CCDC reference number 186/1612.

See http://www.rsc.org/suppdata/dt/1999/3399/ for crystallographic files in .cif format.

### Physical measurements

Infrared spectra were recorded as KBr discs or as Nujol mulls on CsI plates using a Nicolet 510P FTIR spectrophotometer. Elemental analyses (C, H and N) were performed by Atlantic Microlab, Georgia, USA. Fluorine analysis was performed by Desert Analytics, Arizona, USA. Variable-temperature magnetic susceptibility ($\chi_m$) was measured on powdered samples of compounds **1** and **4** with a Quantum Design SQUID Magnetometer operating between 2 and 300 K, and at fields ranging from 10 to 50 kG (1 to 5 T). Samples of **1** and **4** were restrained from torquing in the large magnetic fields by suspending them in molten eicosane (mp 37 °C) which was then allowed to resolidify. Diamagnetic corrections were estimated from Pascal's constants, which were then substracted from the observed

**Table 1** Crystallographic data for complexes **1**·6MeOH, **2**·2MeOH, **3** and **4**

| | **1** | **2** | **3** | **4** |
|---|---|---|---|---|
| Formula | $C_{50}H_{60}Cl_4N_8O_7V_2$ [a] | $C_{24}H_{26}Cl_3CrN_4O_2$ [a] | $C_{28}H_{28.2}ClCu_2N_4O_{9.4}$ [b] | $C_{26}H_{24}F_5BCu_2N_4O_4$ |
| $M$ | 1128.77 | 560.85 | 733.70 | 689.40 |
| Crystal symmetry | Monoclinic | Orthorhombic | Monoclinic | Triclinic |
| Space group | $P2_1/n$ | $Pbca$ | $P2_1/c$ | $P\bar{1}$ |
| $a$/Å | 13.269(2) | 23.106(3) | 7.739(2) | 12.613(2) |
| $b$/Å | 29.629(3) | 8.338(1) | 34.342(7) | 13.380(2) |
| $c$/Å | 14.318(2) | 25.770(3) | 11.052(3) | 9.763(2) |
| $\alpha$/° | | | | 105.41(1) |
| $\beta$/° | 114.93(1) | 90 | 101.77(1) | 110.48(1) |
| $\gamma$/° | | | | 102.89(1) |
| $U$/Å$^3$ | 5104.85 | 4964.63 | 2875.54 | 1393.84 |
| $Z$ | 4 | 8 | 4 | 2 |
| $T$/°C | −172 | −165 | −168 | −170 |
| $D_c$/g cm$^{-3}$ | 1.469 | 1.511 | 1.695 | 1.643 |
| $\mu$/cm$^{-1}$ | 6.349 | 9.564 | 16.361 | 15.996 |
| Unique data | 6684 | 4358 | 5069 | 4906 |
| Observed data | 4874 [c] | 2857 [d] | 3236 [c] | 3541 [d] |
| $R(R')$ | 0.0603 (0.0616) | 0.0543 (0.0427) | 0.0614 (0.0553) | 0.0659 (0.0501) |

[a] Including MeOH solvate molecules. [b] Formula includes components from disordered $OEt^-/OAc^-$ groups. [c] $F > 3\sigma(F)$. [d] $F > 2.33\sigma(F)$.

susceptibilities; the resulting paramagnetic susceptibilities were then fit by the theoretical $\chi_m$ *vs.* T expression as detailed in the text. EPR Measurements were made at X-band frequency (9.4 GHz) on a Bruker ESP 300D spectrometer with a Hewlett-Packard 5350B microwave frequency counter and a Bruker ER 4111 variable-temperature unit. Solution (240–820 nm) electronic spectra were recorded on a Hewlett-Packard 4450A spectrophotometer.

## Results and discussion

### Syntheses

The reaction of $[VCl_3(thf)_3]$ with L in MeOH gave at first an intense red colouration that changed to purple after 2–3 h, and dinuclear $[V_2OCl_2L_2]Cl_2$ **1** was subsequently isolated. The source of the $O^{2-}$ in the product is presumably solvent water impurities, and increased yields of **1** can be obtained by deliberate addition of small amounts of water to the reaction mixture, eqn. (1). Reaction of $[Cr(H_2O)_4Cl_2]Cl{\cdot}2H_2O$ with L in refluxing

$$2\,[VCl_3(thf)_3] + 2\,L + H_2O \longrightarrow [V_2OCl_2L_2]Cl_2 + 2\,HCl + 6\,thf \quad (1)$$

MeOH produced a green solution from which mononuclear *trans*-$[CrCl_2L]Cl$ **2** was isolated after slow evaporation, eqn. (2).

$$[Cr(H_2O)_4Cl_2]Cl{\cdot}2H_2O + L \longrightarrow [CrCl_2L]Cl + 6\,H_2O \quad (2)$$

The same mononuclear product was obtained using $[CrCl_3(thf)_3]$[12] as starting material. Thus the hypothetical $[Cr_2OCl_2L_2]Cl_2$, analogous to **1**, does not form under these conditions. Attempts deliberately to introduce a bridging $O^{2-}$ in the chromium system by alternative means have not been pursued.

The reaction of L with a copper(II) source was previously investigated by others and the mononuclear species $[CuL][ClO_4]_2$ obtained.[6] In a similar reaction but using a Cu : L ratio of 2 : 1 the dinuclear complex $[Cu_2(OAc)_{2.4}(OEt)_{0.6}L]ClO_4$ **3** was obtained as a minor product along with the known mononuclear compound. These were conveniently separated by their differing colour and solubility in MeCN, but the yields of **3** were low (<20%). Attempts to increase the yield by addition of MeCN to the reaction mixture (to prevent precipitation of the blue mononuclear species) gave only green crystals. The IR analysis closely resembles that of **3** with the absence of the peak at 1668 cm$^{-1}$ from the mondentate $OAc^-$. The $OAc^-/OEt^-$ disorder present in **3** suggests an equilibrium between the bridging $OAc^-$ and the reaction solvent EtOH; however, the above evidence suggests that mixed MeCN–EtOH solvent systems give a similar dinuclear structure but with only bridging $OEt^-$.

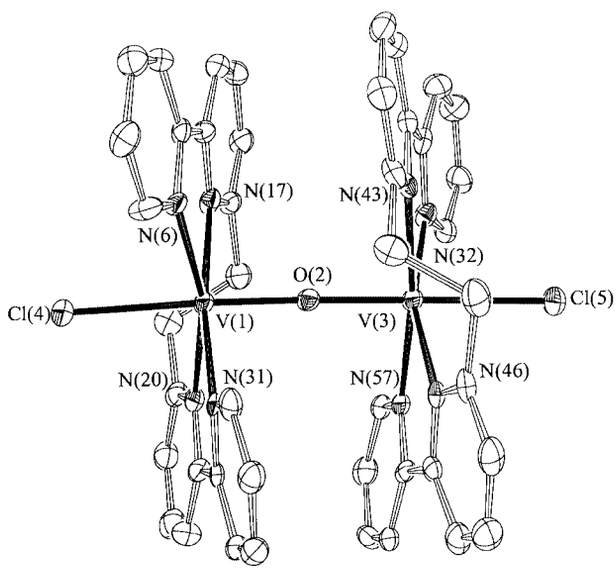


**Fig. 1** An ORTEP representation of the cation of complex **1**. Thermal ellipsoids (as in all the Figures) are at the 50% probability level.

In an attempt to protonate one of the bridging acetate ligands in compound **3** addition of one equivalent of $HBF_4$ was carried out, and this was instead found to give the fluoro-bridged complex $[Cu_2F(OAc)_2L]BF_4$ **4** with a $[Cu_2(\mu\text{-}F)(\mu\text{-}OAc)_2]^+$ core. This is a new structural type in $Cu^{II}/F$ chemistry, the previous examples containing a $[Cu_2(\mu\text{-}F)_2]^{2+}$ [13a–d] or a $[Cu_2(\mu\text{-}F)]^{3+}$ core.[13e] The source of the $F^-$ bridge undoubtedly comes from the $BF_4^-$ anion; although the mechanism for this is not known it likely involves displacement of $F^-$ by $OAc^-$ to give $F_3BOAc^-$. Several other copper(II) fluoride species are known where the source of the $F^-$ ions was $BF_4^-$ or $PF_6^-$ anions.[13] Increased amounts of $HBF_4$ were added in an attempt to increase the yield but this instead led to a mixture of blue-green crystals of **4** and the blue mononuclear species $[CuL][BF_4]_2$.

### Crystal structures

The ORTEP[14] representations of the cations **1**–**4** are shown in Figs. 1–6. The core of **3** is shown in Fig. 4. The interaction between neighbouring molecules in **4** is shown in Fig. 6. Selected interatomic distances and angles are listed in Tables 2–5.

**Table 2** Selected bond distances (Å) and angles (°) for $[V_2OCl_2L_2]Cl_2$ **1**

| | | | |
|---|---|---|---|
| V(1)···V(3) | 3.583(1) | V(3)–Cl(5) | 2.418(1) |
| V(1)–Cl(4) | 2.402(1) | V(3)–O(2) | 1.794(2) |
| V(1)–O(2) | 1.789(2) | V(3)–N(32) | 2.153(3) |
| V(1)–N(6) | 2.158(3) | V(3)–N(43) | 2.203(3) |
| V(1)–N(17) | 2.200(2) | V(3)–N(46) | 2.180(3) |
| V(1)–N(20) | 2.177(4) | V(3)–N(57) | 2.190(3) |
| V(1)–N(31) | 2.168(3) | | |
| | | | |
| V(1)–O(2)–V(3) | 178.20(3) | Cl(5)–V(3)–O(2) | 179.20(11) |
| Cl(4)–V(1)–O(2) | 176.90(10) | Cl(5)–V(3)–N(32) | 81.48(8) |
| Cl(4)–V(1)–N(6) | 82.42(8) | Cl(5)–V(3)–N(43) | 94.80(8) |
| Cl(4)–V(1)–N(17) | 94.78(8) | Cl(5)–V(3)–N(46) | 81.86(7) |
| Cl(4)–V(1)–N(20) | 81.14(7) | Cl(5)–V(3)–N(57) | 92.57(7) |
| Cl(4)–V(1)–N(31) | 92.58(7) | O(2)–V(3)–N(32) | 99.30(11) |
| O(2)–V(1)–N(6) | 100.67(12) | O(2)–V(3)–N(43) | 85.27(10) |
| O(2)–V(1)–N(17) | 86.25(9) | O(2)–V(3)–N(46) | 97.36(10) |
| O(2)–V(1)–N(20) | 95.77(11) | O(2)–V(3)–N(57) | 87.40(11) |
| O(2)–V(1)–N(31) | 86.55(9) | N(32)–V(3)–N(43) | 75.00(14) |
| N(6)–V(1)–N(17) | 75.21(14) | N(32)–V(3)–N(46) | 163.29(9) |
| N(6)–V(1)–N(20) | 163.48(9) | N(32)–V(3)–N(57) | 103.80(15) |
| N(6)–V(1)–N(31) | 102.80(16) | N(43)–V(3)–N(46) | 107.68(16) |
| N(17)–V(1)–N(20) | 107.77(16) | N(43)–V(3)–N(57) | 172.26(12) |
| N(17)–V(1)–N(31) | 172.03(14) | N(46)–V(3)–N(57) | 75.73(16) |
| N(20)–V(1)–N(31) | 76.40(16) | | |

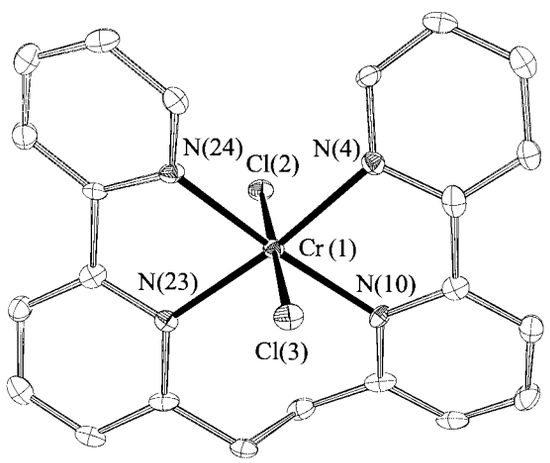


**Fig. 2** An ORTEP representation of the cation of complex **2**.

The cation in compound **1**·6MeOH consists of an oxo-bridged dinuclear species with a near linear V–O–V unit [178.20(3)°] and a $V^{III}\cdots V^{III}$ separation of 3.583(1) Å. Each $V^{III}$ has approximately octahedral co-ordination with the ligand L co-ordinating in an equatorial fashion, and a terminal Cl *trans* to the bridging oxo-group. The limited flexibility of the ethylene linkage between each L ligand's two bpy groups causes the latter to not be coplanar, as is evident from the viewpoint of Fig. 1. The cation has virtual $C_2$ symmetry. The corresponding bpy complex $[V_2OCl_2(bpy)_4]Cl_2$ has a similar $[V–O–V]^{4+}$ core with a $V^{III}\cdots V^{III}$ distance of 3.568 Å and a V–O–V angle of 173.5°,[15] similar to the values found in **1**. The most significant difference between the two compounds is the imposed *trans* arrangement of bpy groups in **1** due to the restraining ethylene linkage in L. This then leads to terminal $Cl^-$ ions that are *trans* to the bridging oxo-group and an average V–Cl distance of 2.410 Å. In contrast, $[V_2OCl_2(bpy)_4]Cl_2$ has a *cis* arrangement of bpy ligands, $Cl^-$ ions *cis* to the bridging oxo-group, and a shorter V–Cl distance [2.381(2) Å]. The corresponding phenanthroline complex $[V_2OCl_2(phen)_4]Cl_2$ also has *cis* orientation of ligands.[16]

The cation in compound **2**·2MeOH consists of a six-co-ordinate chromium(III) ion bound to four N donor atoms from L and two $Cl^-$ ions that are *trans* (Fig. 2). The largest deviation from octahedral geometry is the elongated Cr–N distances to N(10) and N(23) [average 2.113(4) Å] compared with those to N(4) and N(24) [average 2.071(4) Å], which can be attributed to the ethylene bridge in L. This is further supported by the increased *cis* angle of 107.85° for N(10)–Cr(1)–N(23). A similar difference in bond lengths is seen in the square planar $[CuL]^{2+}$ cation.[6] A similar *trans* arrangement of N donors in a tetradentate ligand has been reported previously utilising a quaterpyridine ligand.[17] In contrast, several mononuclear chromium(III) complexes containing two bpy groups all have a *cis* arrangement of bpy ligands, *e.g.* $[Cr(bpy)_2(H_2O)Cl][ClO_4]_2$.[18]

The cation in compound **3** consists of two $Cu^{II}$ ions separated by 3.214(3) Å that are bridged by two acetate ligands in a $\eta^1:\eta^1$ bridging mode and a bridging oxygen atom common to a third monoatomic bridging acetate as well as an ethoxide (Fig. 3). The individual $OAc^-/OEt^-$ components were refined to a

**Table 3** Selected bond distances (Å) and angles (°) for $[CrCl_2L]Cl$·2MeOH **2**·2MeOH

| | | | |
|---|---|---|---|
| Cr(1)–Cl(2) | 2.298(2) | Cr(1)–N(10) | 2.113(4) |
| Cr(1)–Cl(3) | 2.291(2) | Cr(1)–N(23) | 2.112(4) |
| Cr(1)–N(4) | 2.071(4) | Cr(1)–N(24) | 2.072(4) |
| | | | |
| Cl(2)–Cr(1)–Cl(3) | 179.58(7) | Cl(3)–Cr(1)–N(24) | 88.64(14) |
| Cl(2)–Cr(1)–N(4) | 87.95(14) | N(4)–Cr(1)–N(10) | 77.28(16) |
| Cl(2)–Cr(1)–N(10) | 91.46(13) | N(4)–Cr(1)–N(23) | 173.71(18) |
| Cl(2)–Cr(1)–N(23) | 88.27(12) | N(4)–Cr(1)–N(24) | 97.83(15) |
| Cl(2)–Cr(1)–N(24) | 91.71(14) | N(10)–Cr(1)–N(23) | 107.85(15) |
| Cl(3)–Cr(1)–N(4) | 92.23(14) | N(10)–Cr(1)–N(24) | 174.07(17) |
| Cl(3)–Cr(1)–N(10) | 88.21(13) | N(23)–Cr(1)–N(24) | 77.26(16) |
| Cl(3)–Cr(1)–N(23) | 91.58(13) | | |

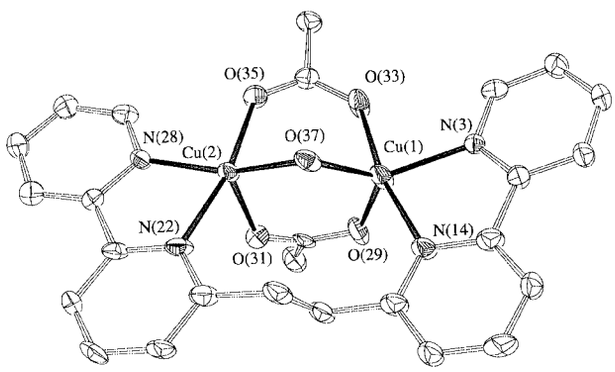


**Fig. 3** An ORTEP representation of the cation of complex **3**. The disordered $OEt^-/OAc^-$ atoms sharing O(37) are removed for clarity; see Fig. 4.

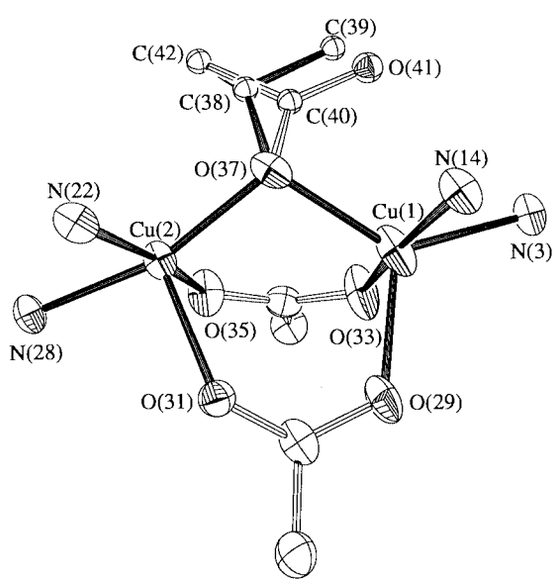


**Fig. 4** An ORTEP representation of the core of complex **3**. The disordered $OEt^-$ (60%) and $OAc^-$ (40%) components are included.

**Table 4** Selected bond distances (Å) and angles (°) for $[Cu_2(OAc)_{2.4}(OEt)_{0.6}L]ClO_4$ **3**

| | | | |
|---|---|---|---|
| Cu(1)···Cu(2) | 3.214(3) | Cu(2)–O(37) | 1.950(5) |
| Cu(1)–O(29) | 2.092(5) | Cu(2)–N(22) | 2.082(6) |
| Cu(1)–O(33) | 1.942(5) | Cu(2)–N(28) | 1.989(6) |
| Cu(1)–O(37) | 2.024(5) | O(37)–C(40) | 1.249(20) |
| Cu(1)–N(3) | 2.043(6) | C(40)–O(41) | 1.243(27) |
| Cu(1)–N(14) | 2.018(5) | C(40)–C(42) | 1.505(26) |
| Cu(2)–O(31) | 2.168(4) | O(37)–C(38) | 1.516(14) |
| Cu(2)–O(35) | 1.995(5) | C(38)–C(39) | 1.492(22) |
| | | | |
| Cu(1)–O(37)–Cu(2) | 107.94(22) | O(31)–Cu(2)–O(37) | 103.41(21) |
| O(29)–Cu(1)–O(33) | 88.00(22) | O(31)–Cu(2)–N(22) | 92.59(21) |
| O(29)–Cu(1)–O(37) | 115.46(22) | O(31)–Cu(2)–N(28) | 96.08(22) |
| O(29)–Cu(1)–N(3) | 114.39(23) | O(35)–Cu(2)–O(37) | 87.58(21) |
| O(29)–Cu(1)–N(14) | 98.45(22) | O(35)–Cu(2)–N(22) | 168.24(24) |
| O(33)–Cu(1)–O(37) | 91.48(21) | O(35)–Cu(2)–N(28) | 88.19(23) |
| O(33)–Cu(1)–N(3) | 88.10(23) | O(37)–Cu(2)–N(22) | 101.06(22) |
| O(33)–Cu(1)–N(14) | 168.65(27) | O(37)–Cu(2)–N(28) | 160.25(22) |
| O(37)–Cu(1)–N(3) | 130.10(22) | N(22)–Cu(2)–N(28) | 80.99(24) |
| O(37)–Cu(1)–N(14) | 94.12(23) | O(37)–C(40)–O(41) | 129.8(21) |
| N(3)–Cu(1)–N(14) | 80.73(25) | O(37)–C(40)–C(42) | 109.8(19) |
| O(31)–Cu(2)–O(35) | 93.13(19) | O(37)–C(38)–C(39) | 110.2(13) |

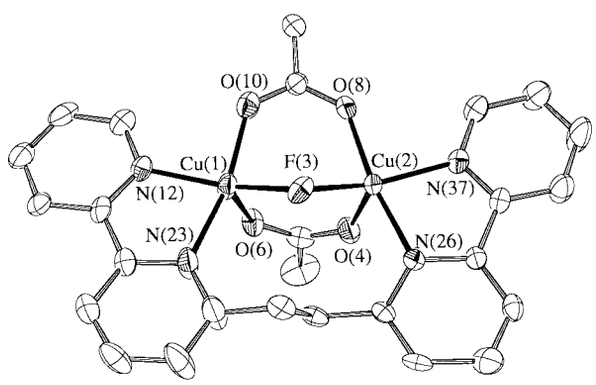


**Fig. 5** An ORTEP representation of the cation of complex **4**.

40:60 ratio, and the disorder is shown in Fig. 4. The angle at the bridging oxygen is 107.94(22)° [Cu(1)–O(37)–Cu(2)]. The ligand L bridges across the dinuclear core and completes five-co-ordination at each $Cu^{II}$. The geometry at each $Cu^{II}$ is quite different and analysis of the shape-determining angles using the approach of Addison *et al.*[19] yields $\tau$ values of 0.65 for Cu(1) and 0.14 for Cu(2) [$\tau = 0$ and 1 for ideal square pyramidal and trigonal bipyramidal geometries, respectively]. Therefore Cu(2) approximates well to square pyramidal geometry with O(31) at the apex, and Cu(1) is closer to trigonal bipyramidal albeit a severely distorted one [O(33)–Cu(1)–N(14) 168.65(27)°]. These geometries are further supported by the relatively long Cu(2)–O(31) bond [2.168(4) Å] at the apex in Cu(2), whereas Cu(1) has a range of bond lengths [1.942(5)–2.092(5) Å] with no apparent trend. An additional weak interaction between Cu(1) and the non-bridging oxygen of the monodentate acetate is observed [Cu(1)···O(41) 2.77(2) Å].

The reaction chemistry of $[Cu_2(OAc)_4(H_2O)_2]$ with bpy has been extensively investigated and many dinuclear systems as well as trinuclear and polymeric species have been synthesized.[20] Previous work in this group has led to the dinuclear complexes $[Cu_2(OAc)_3(bpy)_2]ClO_4$ and $[Cu_2(OAc)_2(OEt)(bpy)_2]PF_6$ whose cations are very similar to that found in **3**.[21] In fact a hybrid of these two complexes with $[Cu_2(OAc)_3]^+$ and $[Cu_2(OAc)_2(OEt)]^+$ cores represents the disorder apparent in **3**. The Cu···Cu distances of 3.392(1) and 3.230(1) Å in the monodentate acetate and ethoxide bridged complexes, respectively, are slightly longer than in **3** [3.214(3) Å], which may represent the effect of the ethylene linkage between the two bpy units in L.

The $[Cu_2F(OAc)_2]^+$ cation in compound **4** is very similar to

**Table 5** Selected bond distances (Å) and angles (°) for $[Cu_2F(OAc)_2L]BF_4$ **4**

| | | | |
|---|---|---|---|
| Cu(1)···Cu(2) | 3.248(2) | Cu(2)–F(3) | 1.933(3) |
| Cu(1)–F(3) | 1.916(3) | Cu(2)–O(4) | 2.149(5) |
| Cu(1)–O(6) | 2.171(4) | Cu(2)–O(8) | 1.959(5) |
| Cu(1)–O(10) | 1.943(4) | Cu(2)–N(26) | 2.032(6) |
| Cu(1)–N(12) | 1.996(5) | Cu(2)–N(37) | 1.988(5) |
| Cu(1)–N(23) | 2.038(5) | | |
| | | | |
| Cu(1)–F(3)–Cu(2) | 115.12(16) | F(3)–Cu(2)–O(4) | 103.59(15) |
| F(3)–Cu(1)–O(6) | 103.69(14) | F(3)–Cu(2)–O(8) | 89.86(18) |
| F(3)–Cu(1)–O(10) | 88.91(16) | F(3)–Cu(2)–N(26) | 95.20(20) |
| F(3)–Cu(1)–N(12) | 157.34(16) | F(3)–Cu(2)–N(37) | 151.63(17) |
| F(3)–Cu(1)–N(23) | 95.98(18) | O(4)–Cu(2)–O(8) | 93.95(21) |
| O(6)–Cu(1)–O(10) | 93.88(17) | O(4)–Cu(2)–N(26) | 91.79(23) |
| O(6)–Cu(1)–N(12) | 98.97(17) | O(4)–Cu(2)–N(37) | 104.65(17) |
| O(6)–Cu(1)–N(23) | 97.61(21) | O(8)–Cu(2)–N(26) | 171.26(21) |
| O(10)–Cu(1)–N(12) | 89.19(19) | O(8)–Cu(2)–N(37) | 90.87(20) |
| O(10)–Cu(1)–N(23) | 166.05(20) | N(26)–Cu(2)–N(37) | 81.29(22) |
| N(12)–Cu(1)–N(23) | 81.26(21) | | |

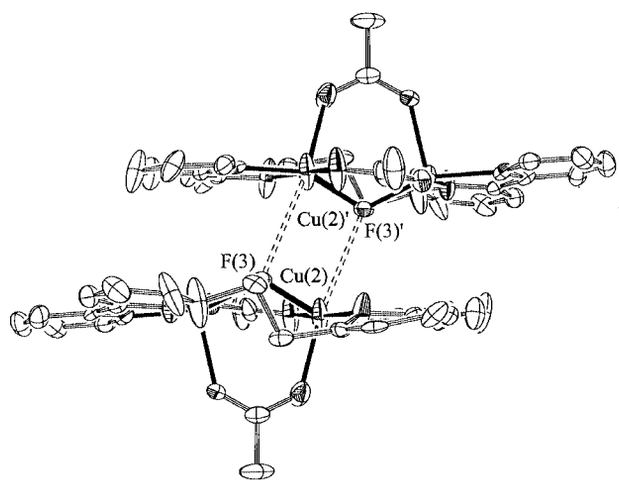


**Fig. 6** An ORTEP representation showing nearest neighbour Cu···F contacts between dinuclear units in compound **4**.

the core structure in **3** with replacement of the $OEt^-/OAc^-$ bridge by a $F^-$ atom (Fig. 5). The Cu···Cu separation of 3.248(2) Å is longer than that in **3** and the Cu–F–Cu bridging angle [115.12(16)°] is larger by 7° than the corresponding bridging Cu–O–Cu angle in **3**. Unlike complex **3**, the geometry at each $Cu^{II}$ is very similar and both Cu(1) and Cu(2) can be described as square pyramidal ($\tau = 0.15$ and 0.33 respectively) with O(6) and O(4) at the apical positions. The closest intermolecular interactions in **4** are Cu···F contacts [3.116 Å] between neighbouring $[Cu_2F(OAc)_2L]^+$ units arranged in a head-to-head fashion (Fig. 6). This is a very weak interaction and is appreciably longer than the sum of the respective van der Waals radii [2.9–3.0 Å]. This kind of linking of dinuclear units has been observed previously in the tetranuclear species $[Mn_4O_2(OAc)_4L_2][ClO_4]_2$,[8] although the interdimer Mn···O interactions are stronger than the Cu···F interactions, and the manganese species is better described as a tetranuclear complex.

## Magnetic susceptibility studies

Variable-temperature magnetic susceptibility studies were performed on powdered samples of complexes **1** and **4** in the temperature range 2.0–300.0 K. For **1** the effective magnetic moment ($\mu_{eff}$) per $V_2$ molecule increases slightly from 4.83 $\mu_B$ at 300 K to 4.86 $\mu_B$ at 50 K, and then decreases slightly to 4.83 $\mu_B$ at 15 K (Fig. 7). Below 15 K, $\mu_{eff}$ decreases more rapidly to a value of 4.26 $\mu_B$ at 2.00 K. The value of $\mu_{eff}$ for two non-interacting vanadium(III) ions is 4.00 $\mu_B$, whereas the observed

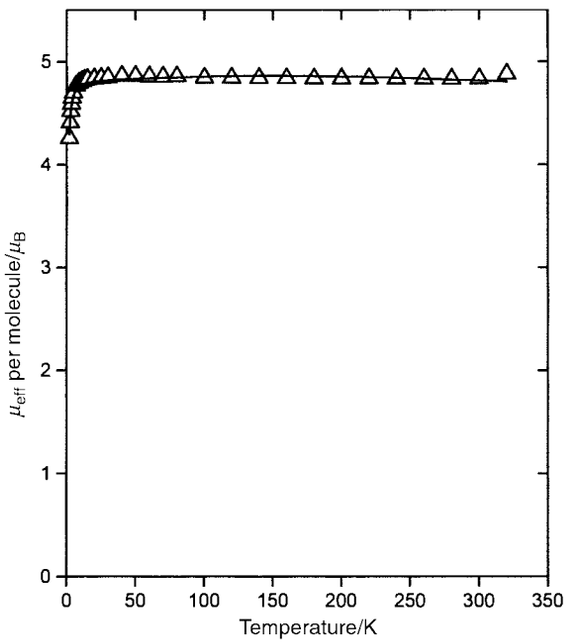


**Fig. 7** Plot of effective magnetic moment ($\mu_{eff}$) per $V_2$ molecule *vs.* temperature for $[V_2OCl_2L_2]Cl_2$ **1**. The solid line is a least-squares fit of the experimental data to the appropriate theoretical expression. See the text for the fitting parameters.

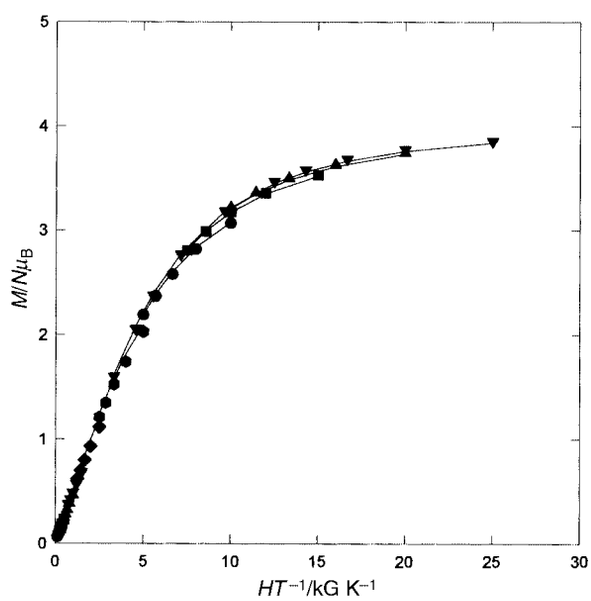


**Fig. 8** Plot of reduced magnetisation ($M/N\mu_B$) *vs.* $H/T$ for complex **1** in applied fields between 0.5 and 50.0 kG.

moment is very close to that expected for an $S = 2$ state (4.90 $\mu_B$ with $g = 2$). The behaviour is clearly indicative of intramolecular ferromagnetic exchange interactions. The drop in $\mu_{eff}$ below 15 K is assigned to the effects of zero-field splitting and/or weak intermolecular, antiferromagnetic interactions. In order to confirm and probe the ground state further, magnetisation data were collected at various fields in the 10–50 kG range. The data are plotted in Fig. 8 as reduced magnetization ($M/N\mu_B$) *versus* $H/T$. At the highest fields and lowest temperature (2.00 K) the data approach the value of 4 expected for an $S = 2$ state with $g = 2.0$. A spin Hamiltonian, eqn. (3), was

$$H = \beta H_z(g_1S_{1z} + g_2S_{2z}) - 2JS_1S_2 + D_1(S_{2z}^2 - \tfrac{1}{3}S_1(S_1 + 1)) + D_2(S_{2z}^2 - \tfrac{1}{3}S_2(S_2 + 1)) \quad (3)$$

constructed in the limit of an isotropic Zeeman interaction and

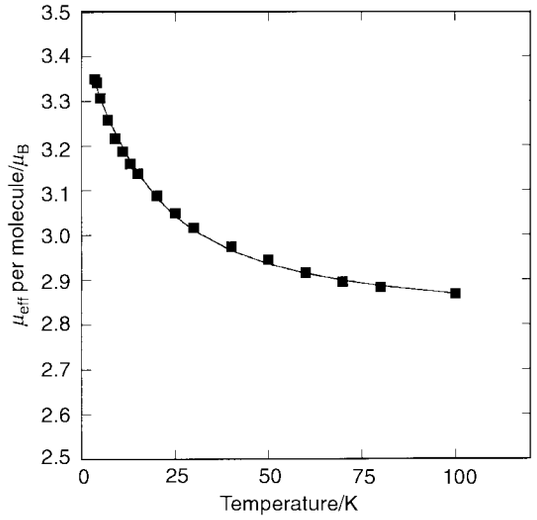


**Fig. 9** Plot of effective magnetic moment ($\mu_{eff}$) per $Cu_2$ molecule *vs.* temperature for $[Cu_2F(OAc)_2L]BF_4$ **4**. The solid line is a fit of the experimental data by the Bleaney–Bowers equation. Only the 3.50 to 100 K data are shown. See the text for fitting parameters.

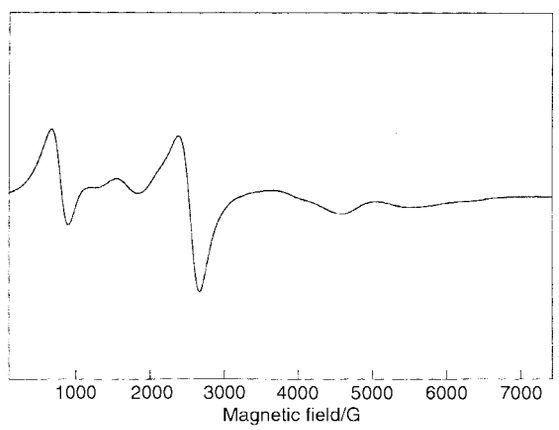


**Fig. 10** X-Band EPR spectrum at 100 K of a polycrystalline sample of $[Cu_2F(OAc)_2L]BF_4$ **4**.

axial zero-field splitting interaction for **1**. Each $V^{III}$ has its respective $g$ factor and single-ion axial zero-field splitting parameter ($D$), with the other terms having their usual meanings. The five parameters for the above equation were reduced to three by using the approximate $C_2$ symmetry of **1** and setting $g_1 = g_2$ and $D_1 = D_2$. The data were least-squares fit to yield $J = +117$ cm$^{-1}$, $g = 1.98$, $D_1 = D_2 = +0.28$ cm$^{-1}$, with temperature independent paramagnetism (TIP) held at $400 \times 10^{-6}$ emu mol$^{-1}$. This fit indicates that the excited $S = 1$ manifold lies 468 cm$^{-1}$ above the ground $S = 2$ manifold, and even at 300 K very little of this $S = 1$ state is populated. This strong ferromagnetic exchange ($J > 100$ cm$^{-1}$) has been observed for several other vanadium(III) dimers containing the $[V–O–V]^{4+}$ subunit,[22] and a thorough account of the commonly observed ferromagnetic coupling has been given elsewhere.[22b,c]

The effective magnetic moment ($\mu_{eff}$) of complex **4** slowly increased from 2.87 $\mu_B$ at 100 K to a maximum value of 3.35 $\mu_B$ at 3.50 K (Fig. 9), then dropped rapidly to 3.26 $\mu_B$ at 2.00 K. The data collected above 100 K were deemed to be unreliable as the SQUID response from the dinuclear copper(II) centres became of the same order of magnitude as the SQUID response from the sample holder. These data were excluded from fitting procedures. The initial increase in $\mu_{eff}$ is indicative of an intramolecular ferromagnetic interaction ($J > 0$). The expected $\mu_{eff}$ value for two non-interacting copper(II) ions is 2.79 $\mu_B$, whereas the expected $\mu_{eff}$ value for an $S = 1$ state is 3.22 $\mu_B$ if $g = 2.28$. Clearly **4** experiences a ferromagnetic exchange

interaction which results in an $S = 1$ ground state. The drop in $\mu_{eff}$ below 3.5 K likely reflects Boltzmann depopulation effects due to Zeeman splitting. An excellent fit to the data (3.5–100.0 K) was realised by use of the Bleaney–Bowers equation[23] with $J = +7.8(5)$ cm$^{-1}$, $g = 2.28(2)$ and $\theta = +0.26(3)$ K, and this fit is shown as a solid line in Fig. 9. The Weiss constant ($\theta$) was introduced to take into account the weak interdimer exchange interactions that were expected to result from the observed Cu · · · F interdimer bonds in the crystal structure (see above).

The EPR spectrum of a polycrystalline sample of compound **4** at X-band frequency was recorded (Fig. 10). At room temperature a weak signal was obtained with transitions typical of a spin-triplet state. On cooling to 100 K the spectroscopic features were identical but with a marked increase in intensity, and a satisfactory signal-to-noise ratio was obtained on a single scan. Formally forbidden transitions ($\Delta m_S = 2$) were observed at $g_{eff} \approx 4$ (features *ca.* 1500 G) as well as allowed ($\Delta m_S = 1$) transitions typical of a spin-triplet state with small zero-field splitting ($D$). The observed increase in intensity with decreasing temperature is consistent with the above magnetic behaviour of **4**, and an EPR active triplet ground state.

All previous structurally and magnetically characterised copper(II) dinuclear complexes with bridging fluoride contain the $[Cu_2F_2]^{2+}$ unit,[13a–d] and in these cases antiferromagnetic exchange is observed. This contrasts with the ferromagnetic exchange in **4**. Indeed the observed coupling in **4** is similar to that of $[Cu_2(OAc)_3(bpy)_2]ClO_4$,[21a] where structurally the only difference between the two complexes is replacement of a monodentate acetate by fluoride. In $[Cu_2(OAc)_3(bpy)_2]^+$ the ferromagnetic exchange interaction was rationalised as resulting from the non-complementary nature of the overlap between the magnetic orbitals on the $Cu^{2+}$ ions and the bridging ligand orbitals of the appropriate symmetry, *i.e.* the symmetric ($\phi_s$) and antisymmetric ($\phi_a$) combinations of the metal magnetic orbitals have net overlaps with different bridging ligands (see Fig. 9 of ref. 21*a*); thus $\phi_s$ and $\phi_a$ are each destabilised by a different bridging ligand and if the extent of this destabilisation is comparable then they will have similar energies and the ground state will be $S = 2$. In complex **4** the $F^-$-for-monodentate $AcO^-$ bridge has little other effect on the core structure and exactly the same magnetic arguments hold: indeed it would have been unexpected had the coupling not been ferromagnetic in **4**.

## Conclusion

The present study utilising the bis-bipyridyl ligand L has provided mononuclear (Cr) and dinuclear (V and 2 Cu) species different to those previously obtained with the parent bipyridyl chelate. The fluoride bridged complex $[Cu_2F(OAc)_2L]BF_4$ **4** has a $[Cu_2F(OAc)_2]^+$ bridging unit not observed before. Magnetochemical data of **4** clearly show intramolecular ferromagnetic exchange between the copper(II) ions, which contrasts with all previously reported fluoride-bridged copper(II) dimers that have shown antiferromagnetic exchange interactions.[13]

The previously synthesized $Mn_4$,[8] $Fe_6$[9] and $Co_8$[7] complexes with L all incorporate dinuclear subunits that are similar to the core unit found in **3** and **4** with Cu. This suggests a rich source of untapped chemistry with the bis-bipyridyl ligand L and derivatives for the preparation of novel high nuclearity compounds, and further studies are in progress.

## Acknowledgements

This work was supported by the US National Science Foundation.

## References

1 (*a*) D. N. Hendrickson, G. Christou, E. A. Schmitt, E. Libby, J. S. Bashkin, S. Wang, H.-L. Tsai, J. B. Vincent, P. D. W. Boyd, J. C. Huffman, K. Folting, Q. Li and W. E. Streib, *J. Am. Chem. Soc.*, 1992, **114**, 2455; (*b*) J. B. Vincent, C. Christmas, J. C. Huffman, G. Christou, H.-R. Chang, and D. N. Hendrickson, *J. Chem. Soc., Chem. Commun.*, 1987, 236; (*c*) J. B. Vincent, C. Christmas, H.-R. Chang, Q. Li, P. D. W. Boyd, J. C. Huffman, D. N. Hendrickson and G. Christou, *J. Am. Chem. Soc.*, 1989, **111**, 2086.
2 S. P. Perlepes, J. C. Huffman and G. C. Christou, *J. Chem. Soc., Chem. Commun.*, 1991, 1657.
3 H. J. Eppley, S. M. J. Aubin, W. E. Streib, J. C. Bollinger, D. N. Hendrickson and G. Christou, *Inorg. Chem.*, 1997, **36**, 109.
4 (*a*) K. Dimitrou, K. Folting, W. E. Streib and G. Christou, *J. Am. Chem. Soc.*, 1993, **115**, 6432; (*b*) J. A. Bertrand and T. C. Hightower, *Inorg. Chem.*, 1973, **12**, 206.
5 M. A. Halcrow, J. C. Huffman and G. Christou, *Angew. Chem., Int. Ed. Engl.*, 1995, **34**, 889.
6 T. Garber, S. Van Wallendael, D. P. Rillema, M. Kirk, W. E. Hatfield, J. H. Welch and P. Singh, *Inorg. Chem.*, 1990, **29**, 2863.
7 V. A Grillo, Z. Sun, K. Folting, J. C. Bollinger, D. N. Hendrickson and G. Christou, *Chem. Commun.*, 1996, 2233.
8 V. A Grillo, M. J. Knapp, J. C. Bollinger, D. N. Hendrickson and G. Christou, *Angew. Chem., Int. Ed. Engl.*, 1996, **35**, 1818.
9 C. M. Grant, M. J. Knapp, W. E. Streib, J. C. Huffman, D. N. Hendrickson and G. Christou, *Inorg. Chem.*, 1998, **37**, 6065.
10 L. E. Manzer, *Inorg. Synth.* 1982, **21**, 138.
11 (*a*) M. H. Chisholm, K. Folting, J. C. Huffman and C. C. Kirkpatrick, *Inorg. Chem.*, 1984, **23**, 1021; (*b*) G. M. Sheldrick, *SHELXTL/PC Users Manual*, Siemens Analytical X-ray Instruments, Inc., Madison, WI, 1990; (*c*) P. Main, S. J. Fiske, S. E. Hill, L. Lessinger, G. Germain, J.-P. Declerq and M. M. Woolfson, MULTAN 78, Universities of York and Louvain, 1978.
12 J. P. Collman and E. T. Kittleman, *Inorg. Synth.*, 1966, **8**, 149.
13 (*a*) W. C. Velthuizen, J. G. Haasnoot, A. J. Kinneging, F. J. Rietmeijer and J. Reedijk, *J. Chem. Soc., Chem. Commun.*, 1983, 1366; (*b*) F. J. Rietmeijer, R. A. G. de. Graff and J. Reedijk, *Inorg. Chem.*, 1984, **23**, 151; (*c*) R. R. Jacobson, Z. Tyeklàr, K. D. Karlin and J. Zubieta, *Inorg. Chem.*, 1991, **30**, 2035; (*d*) S. C. Lee and R. H. Holm, *Inorg. Chem.*, 1993, **32**, 4745; (*e*) M. Mikuriya, S. Kida and I. Murase, *Bull. Chem. Soc. Jpn.*, 1987, **60**, 1681.
14 C. K. Johnson, ORTEP II, Report ORNL-5138, Oak Ridge National Laboratory, Oak Ridge, TN, 1976.
15 S. G. Brand, N. Edelstein, C. J. Hawkins, G. Shalimoff, M. R. Snow and E. R. T. Tiekink, *Inorg. Chem.*, 1990, **29**, 434.
16 T. Otieno, M. R. Bond, L. M. Mokry, R. B. Walter and C. J. Carrano, *Chem. Commun.*, 1996, 37.
17 E. C. Constable, S. M. Elder and D. A. Tocher, *Polyhedron*, 1992, **11**, 1337.
18 W. A. Wickramasinghe, P. H. Bird, M. A. Jamieson, N. Serpone and M. Maestri, *Inorg. Chim. Acta*, 1982, **64**, L85.
19 A. W. Addison and T. N. Rao, *J. Chem. Soc., Dalton Trans.*, 1984, 1349.
20 (*a*) S. Meenakumari, S. K. Tiwary and A. R. Chakravarty, *Inorg. Chem.*, 1994, **33**, 2085; (*b*) S. P. Perlepes, E. Libby, W. E. Streib, K. Folting and G. Christou, *Polyhedron*, 1992, **11**, 923.
21 (*a*) G. Christou, S. P. Perlepes, E. Libby, K. Folting, J. C. Huffman, R. J. Webb and D. N. Hendrickson, *Inorg. Chem.*, 1990, **29**, 3657; (*b*) S. P. Perlepes, J. C. Huffman and G. Christou, *Polyhedron*, 1992, **12**, 1471.
22 (*a*) P. Knopp, K. Wieghardt, B. Nuber, J. Weiss and W. S. Sheldrick., *Inorg. Chem.*, 1990, **29**, 363; (*b*) P. Knopp and K. Wieghardt, *Inorg. Chem.*, 1991, **30**, 4061; (*c*) M. R. Bond, R. S. Czernuszewicz, B. C. Dave, Q. Yan, M. Mohan, R. Verastegue and C. J. Carrano, *Inorg. Chem.* 1995, **34**, 5857.
23 B. Bleaney and K. D. Bowers, *Proc. R. Soc. London Ser. A*, 1952, **214**, 451.

*Paper 9/05280A*